Manipulation of Nanoneedle and Nanosphere Apatite/Poly(Acrylic Acid) Nanocomposites

Sz-Chian Liou,[1] San-Yuan Chen,[1] Dean-Mo Liu[2]

[1] Department of Materials Science and Engineering, National Chiao Tung University, 1001 Ta-hsueh Road, Hsinchu, Taiwan 300, Republic of China

[2] ApaMatrix Technologies, Incorporated, 58-7151 Moffatt Road, Richmond, British Columbia, Canada V6Y3G9

Received 18 February 2004; revised 18 August 2004; accepted 24 August 2004
Published online 25 January 2005 in Wiley InterScience (www.interscience.wiley.com). DOI: 10.1002/jbm.b.30193

Abstract: Colloidal apatitic nanosphere of 2–5 nm in diameter was synthesized in the presence of poly(acrylic acid), PAA. PAA, which has long been recognized as an inhibitor in the synthesis of hydroxyapatite, is used as a structure-directing agent for the synthesis of calcium-deficient apatite (CDHA) in this study. Experimental observation suggests a critical amount of the low-molecular-weight PAA, above which morphological evolution of CDHA nanoparticles from needle to sphere was observed. This reveals that the PAA acts as an inhibitor for the growth of CDHA crystals. Further incorporation of PAA of high molecular weight formed a highly optically transparent nanocomposite, even with the nanospherical apatite loading up to 35 wt %, suggesting no agglomeration. This was further justified through transmission electron microscopy (TEM), where the CDHA nanospheres were uniformly distributed in the PAA-CDHA nanocomposites. No interfacial crevices were visually observed, indicating a highly compatible interface between the inorganic CDHA and organic PAA phase.

Keywords: calcium-deficient apatite (CDHA); poly(acrylic acid); nanocomposites; nanosphere CDHA

INTRODUCTION

A great advantage of using synthetic apatite is to enhance physiological affinity to the host tissues, or increase biological activity and compatible materials with less biological compatibility due to its chemical and structural similarity to the natural apatite crystals.[1] For most synthetic apatite crystals, the resulting Ca/P ratio is controlled at 1.67, this is called *stoichiometric apatite*. However, in comparison to natural apatite, which has a Ca/P ratio about 1.5, the Ca/P ratio in stoichiometric apatite is higher. The nanometric apatite crystals in the mineral tissues offer superior biological properties to surrounding physiological environment by giving higher metabolic activity than that of synthetic apatite.[1]

Synthesis of apatite crystals have been well documented for decades through a wide variety of methods, including solid-state chemical reaction,[2–4] coprecipitation,[5,6] and sol–gel.[7] Wet chemistry is the most widely used synthetic method to produce micro- to nanocrystalline apatite particles.[8,9] Recently, a number of reports have addressed the *in situ* synthesis of apatite-containing nanocomposites aimed at producing chemically and biologically improved synthetic bones.[10,11] The primary concept is adapted from a naturally occurring process termed *biomimetic process*, where the natural apatite is synthesized in a physiological environment associated with the presence of natural polymer, such as collagen, and ions, which is essentially an *in situ* synthetic process. The prime advantage of the *in situ* synthesis is to produce apatite-based nanocomposites with outstanding chemical and physical homogeneity compared to those derived via conventional mechanical mixing. However, few reports address the occurrence of agglomeration of the nanoapatite particles in the matrix, even through the use of an *in situ* mrthod.[11] Such an agglomeration, although not as extensive as those prepared via mechanical blending, can still adversely affect final properties such as mechanical strength and moduli.[11] Although no further clarification has been made to account for the cause of agglomeration, it is possible to assume that it results from a strong interparticle attraction between the nanoparticles after *in situ* formation. This investigation is an attempt to prepare a CDHA-based nanocomposite with superior homogeneity by using a two-step synthetic process.

Poly(acrylic acid), PAA, has been well documented as a suppressant for the nucleation and growth of apatite crystals

Correspondence to: San-Yuan Chen (e-mail: sychen@cc.nctu.edu.tw)
Contract grant sponsor: National Science Council of the Republic of China; contract grant number: NSC-92-2216-E-009-025

during the course of wet-chemical synthesis and biomimetic formation.[12–14] In recent work, successful synthesis of apatite crystals with controlled aspect ratio (AR = length/diameter) was reported through the use of PAA.[15,16] It is observed that increase in the concentration of PAA polyelectrolyte causes a reduction in the aspect ratio of the resulting apatitic crystals; however, apatite nanocrystals with equiaxial geometry (such as spherelike shape) can rarely be obtained. It is then more interesting to find a method to develop spherical apatite nanocrystals, and a subsequent development of nanocomposite is targeted via the two-step process to be outlined in this study.

EXPERIMENTAL SECTION

Synthesis

The starting materials used in this investigation were analytical-grade reagents $(CH_3COO)_2Ca \cdot xH_2O$ (99%, Aldrich Chemical Company, Inc.) and H_3PO_4 (99%, Riedel-deHaen, Seelze, Germany) as Ca and P precursors, respectively. The Ca solution was prepared by dissolving 0.015, 0.03, and 0.045 mole of $(CH_3COO)_2Ca \cdot xH_2O$ in deionized water. Poly (acrylic acid) (Mw 2000) (PAA, Aldrich Chemical Company, Inc.) (assigned as PAA-2000) with concentrations from 100 to 5000 ppm was added to the Ca solution, and the solution was adjusted to pH 9 with the use of 5*M* NaOH solution. After that, various amounts of phosphoric acid, that is, 0.01, 0.02, and 0.03 mole, was then added dropwise into the solution, with the solutions kept at pH 9 throughout the titration. The white precipitated powder was finally obtained after filtering and washing with deionized water several times. After oven drying at 80°C, the powder, having a Ca/P ratio of 1.5, was determined with the use of atomic absorption spectroscopy.

For nanocomposite synthesis, the CDHA suspensions prepared above were mixed directly with PAA of high molecular weight (Mw 450,000, Aldrich Chemical Company, Inc.) while maintaining the resulting CDHA-PAA suspension at pH 9. The final suspensions with organic high-molecular-weight PAA from 50 to 90 wt % relative to the concentration of the CDHA nanoparticles were obtained. After vigorous stirring for a time span of 16 hours, the suspension, showing an optically transparent appearance, was cast and dried at 100°C, resulting in a highly transparent nanocomposite film.

Structural Analysis

Both the precipitated powder and CDHA-PAA nanocomposite were characterized by transmission electron microscopy (TEM, Philips Tecnai 20, The Netherlands), operating at 200 keV, for nanostructural analysis. The obtained particle size of the CDHA was calculated by averaging more than 500 CDHA particles measured through the TEM images. Both precipitated powder and nanocomposites were characterized with the use of X-ray diffractometer (M18XHF, MAC Science, Tokyo, Japan) to determine the crystalline phase at a scanning rate of 4°(2θ) per min over a 2θ range of 20–60°. Fourier- transform infrared (FTIR) spectra were performed with the use of KBr pellets (2 mg per 300 mg KBr) on a spectrometer (Model 580, Perkin-Elmer) with a resolution of 4.00 cm^{-1}. Infrared spectra were recorded in the range of 4000–400 cm^{-1} to evaluate the molecular structure.

TABLE I. Observation on the Appearance of PAA-Apatite Colloidal Suspensions and Corresponding Particle Dimensions (nm) in Terms of Precursor and PAA (Mw = 2000) Concentrations Used

PAA-2000 concentrations	Precursor concentrations		
	1 x	2 x	3 x
100 ppm	W 20–25 nm 3 nm	W 30 nm 5 nm	W 20 nm 3 nm
500 ppm	W 15–20 nm 3 nm	W 25 nm 3 nm	W 25 nm 3 nm
1000 ppm	W 15 nm 3 nm	W 15 nm 3 nm	W 15 nm 3 nm
5000 ppm	T 5–10 nm	T 5–10 nm	T 5–10 nm

Note: W means the resulting solution showing white, precipitate appearance, where resulting apatite particles are needle shaped; T means the resulting solution showing clear appearance, where the apatite particles are spherical.

RESULTS AND DISCUSSION

The appearance of the resulting suspensions and corresponding particle morphology in terms of the concentration of the starting precursor and the PAA polyelectrolyte (assigned as PAA-2000) were examined and shown in Table I, where the symbol "T" indicates that the solution remains optically clear, and "W" indicates formation of white precipitate. Corresponding particle dimensions were also measured and tabulated. It is clear from Table I that irrespective of the difference in precursor concentrations, that is, double (2×) and triple (3×), a white appearance of the solution is always associated with the presence of needle-like particles, and the suspension with spherical particles presents an optically clear appearance. The needle-shaped particles are typically in the range of 3–5 nm in diameter and 20–30 nm in length [Figure 1(a)], and the spherical particles shape are 5–10 nm in diameter [Figure 1(b)]. These dimensions are much smaller than visible wavelength, so they are supposed to be optically transparent with respect to the visible light; however, the white appearance for solutions containing needle-like particles indicates a strong agglomeration taking place upon synthesis. The opacity of the resulting solution indicates extensive particle agglomeration, causing pronounced light scattering. Such agglomeration usually leads to undesirable properties in final products, as has been previously reported.[14,15]

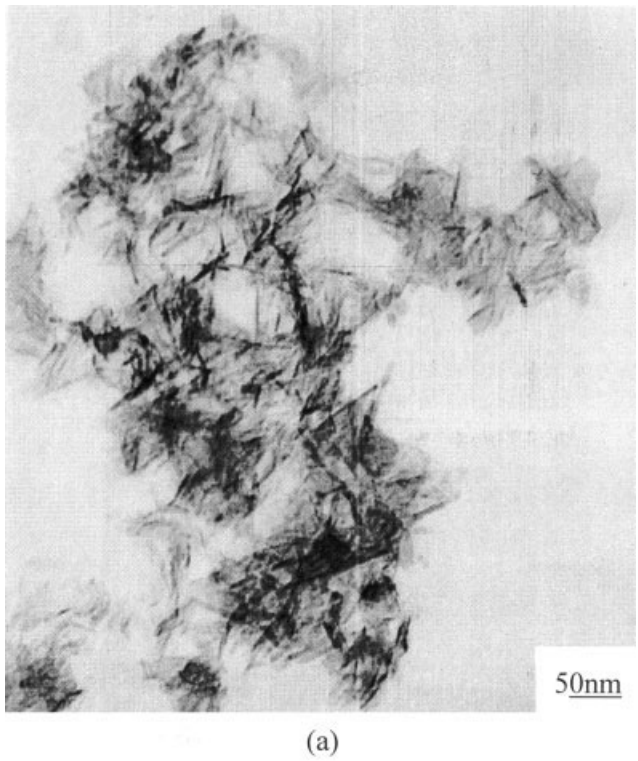

Figure 1. Colloidal apatite prepared in the presence of (a) 100-ppm and (b) 5000-ppm low-molecular-weight ionized PAA, where a significant change in morphological evolution can be observed—(a) needle like and (b) spherical shape.

This is virtually beyond the scope of this investigation, where an agglomerate-free suspension, together with corresponding nanocomposites to be synthesized in-situ, is the main goal.

In contrast, the suspensions with spherical particles, showing an optically transparent appearance, suggest that the particle size is well below the visible regime, including agglomerates that may form in the solution. Transmission electron microscopy (TEM) examination showed that the spherical particles fall in the range of 5–10 nm in diameter, and some larger particles (20–30 nm in diameter) are also detectable; however, it seems that few agglomerates were found in this synthetic scheme.

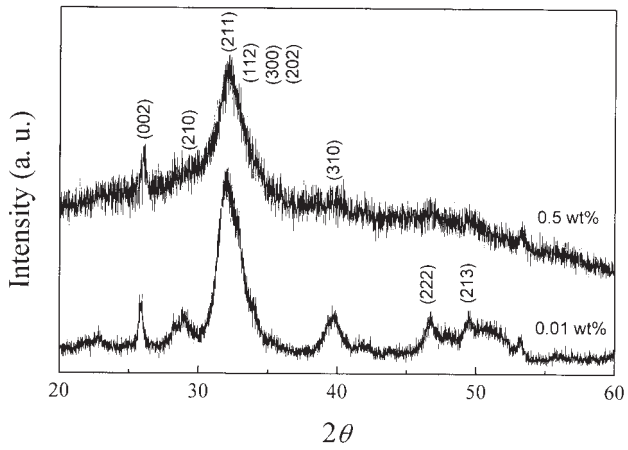

Figure 2. XRD patterns of the colloidal apatite prepared in the presence of low-concentration (bottom curve) and high-concentration (top curve) PAA-2000 polyelectrolyte.

Figures 2 and 3 illustrate the XRD and FTIR spectra of the synthetic apatite powder, respectively. The XRD patterns show that the nanoparticles synthesized in the presence of low (100 ppm) and high (5000 ppm) PAA-2000 polyelectrolyte are characterized as apatitic structures according to the ICDD No. 9-432. FTIR further reveals the characteristic apatitic PO_4^{3-} $\nu 4$ modes in the regime of 600–500 cm^{-1} and PO_4^{3-} $\nu 1$ and $\nu 3$ modes of 1150–1000 cm^{-1}, for both types of nanoparticles.[15,16] These structural observations indicate that the synthesized nanoparticles, regardless of the geometry, have an apatitic structure and can be assigned as a calcium-deficient apatite (CDHA) where Ca/P = 1.5, as

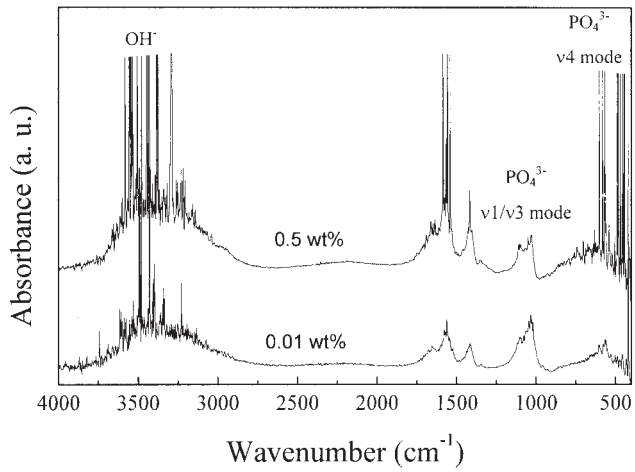

Figure 3. FTIR spectra of the colloidal apatite prepared in the presence of low-concentration (bottom curve) and high-concentration (top curve) PAA-2000 polyelectrolyte.

analytically determined. However, the one with high concentration of PAA-2000 (5000 ppm) appears amorphous-like, with higher diffraction background and decreased relative intensity of the diffraction peaks compared to that derived from low concentration of PAA-2000 (100 ppm). This indicates that the spherical CDHA particles present more disorder structure than those needle-like CDHA, which accordingly suggests that spherical CDHA nanoparticles are more dispersive.

Because the concentration of the PAA-2000 polyelectrolyte is the only parameter for the CDHA nanoparticle synthesis, it is conceivable that it is responsible for the evolution of particle geometry from needle-like to spherical with increasing PAA-2000, that is, from 100 to 5000 ppm. A previous study proposed a preferential adsorption of the ionized PAA molecules (Mw 450,000) onto the c axis of the developing CDHA crystals, resulting in a reduction in the aspect ratio (AR = length/diameter) of the synthesized particles.[15] Similar rationale to the preferential adsorption should be more effectively applied with the use of smaller, ionized PAA-2000 molecules.[16] For a given surface of the CDHA nucleus, higher density of the ionized PAA-2000 is expected and should be more densely packed onto the surface of the growing nuclei than using large molecules. Therefore, a micelle-like structure, as schematically shown in Figure 4, is expected to form.

Moreover, a possible hindrance effect for those larger macromolecules upon adsorption to solid surface can be considerably reduced for smaller molecules. As a result, more efficient adsorption can be expected for the PAA-2000 polyelectrolyte than for PAA-450000 macromolecules. Structural evolution based on such a micelle-like adsorption configuration has resulted in the final particles with smaller size and greater quantity in a given amount of chemical reactant. On the other hand, once the nuclei are subject to growth, a rapid adsorption of the small, ionized PAA-2000 onto the growing nuclei would effectively inhibit preferential growth of the crystals. In turn, a slow and isotropic growth of the crystals likely dominates, resulting in spherical morphology. The relative concentration of PAA-2000 polyelectrolyte to CDHA for the elimination of the preferential growth of the CDHA crystals is estimated in the range of 1000–1700 ppm, as deduced from Table I. Such a dense surface adsorption also provides an explanation for the stability of the suspension, whereas over several months little sedimentation has been visually detected.

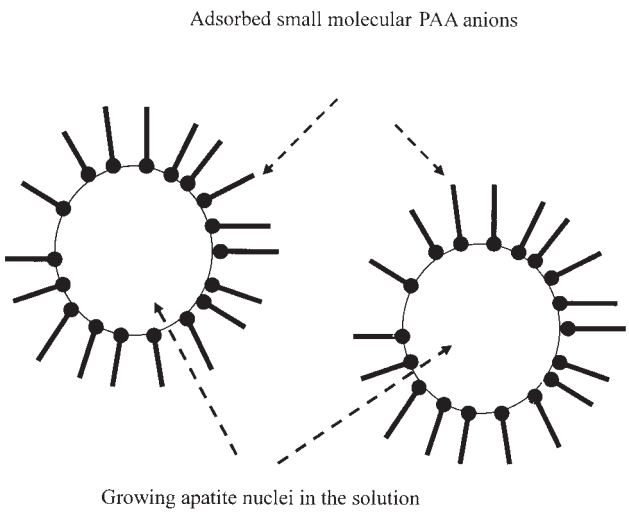

Figure 4. Schematic drawing of the ionized small molecular PAA adsorbed onto the surface of growing apatite nuclei, where a dense surface adsorption leads to the formation of the micelle-like structure. Further growth of the apatite can be highly retarded, resulting in the formation of spherical apatite nanoparticles.

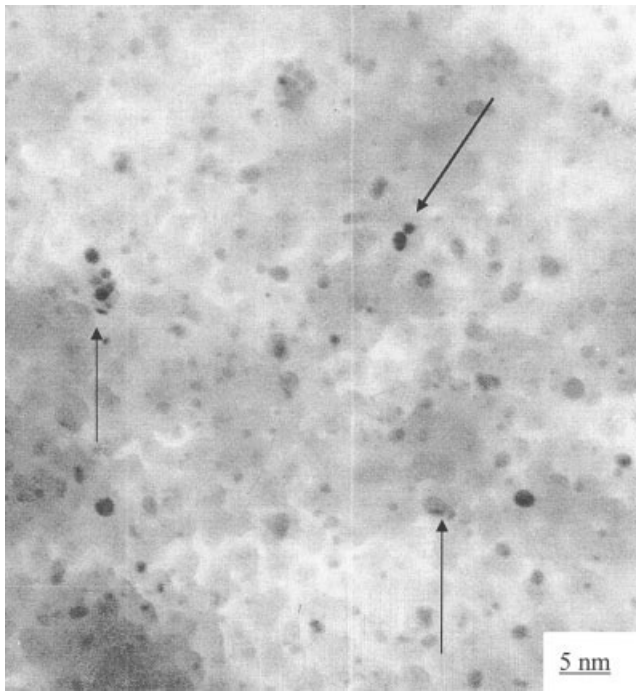

Figure 5. TEM micrograph of the PAA-CDHA nancomposites with numerous agglomerates detectable, where the transparent nature of the nanocomposite disappeared because of extensive agglomeration upon consolidation.

For nanocomposite synthesis, vigorous mixing between the obtained CDHA suspension and PAA-450000 polymer solution was easily carried out and both phases were intimately miscible. without any detectable phase separation. The resulting PAA-CDHA nanocomposites with various concentrations of the CDHA phase from 4 to 71 wt % were successfully synthesized. However, the appearance of the nanocomposites is changing from optically transparent to translucent when the CDHA concentration is greater than about 35 wt %, suggesting that a certain degree of agglomeration may occur at a higher CDHA concentration. This is further evidenced in Figure 5, where larger agglomerates were clearly detected with arrows indicated. The transparent nature of the resulting PAA-CDHA nancomposites also indicates that the degree of dispersion of the CDHA nanospheres remains unchanged from initial suspension synthesis to final composite formation, and this phenomenon has not

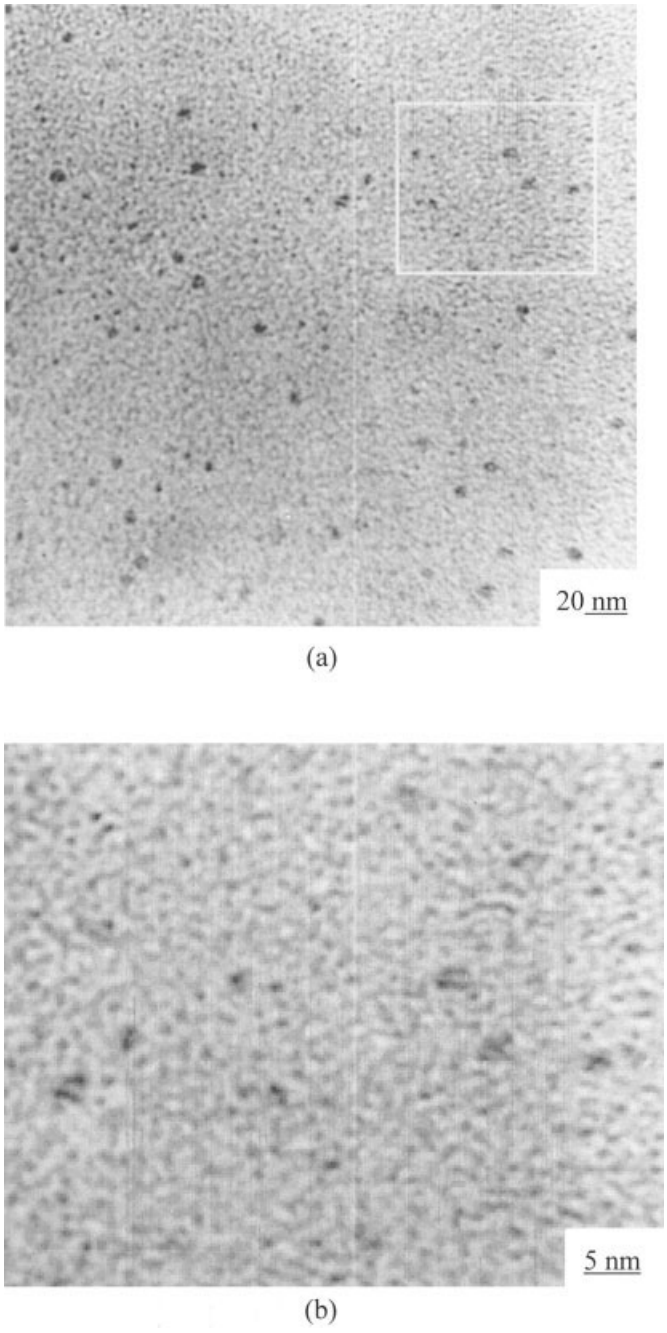

Figure 6. (a) High-resolution TEM micrograph of the transparent PAA-CDHA nanocomposites with well-dispersed CDHA nanospheres detected. (b) Closer examination of the nanostructure of the nanocomposite shown in inset of (a) reveals exceptionally good homogeneity of the nanocomposites with CDHA sizes ranging from 2–5 nm in diameter.

yet been observed in related studies as far as is known. However, particle agglomeration tends to form for higher solid concentration, that is, above 35 wt %, when the water is gradually removed upon ambient drying. Such particle agglomeration is then considered as percolation that thresholds at a critical solid concentration of about 35% in the suspension currently under investigation.

Figure 6(a) is a high-resolution TEM observation on a selected nanocomposite with 30 wt % solid concentration. Nanospheres with particle sizes ranging from 5–10 nm are sparsely dispersed within the PAA-450000 polymeric matrix. However, an enlargement of marked region in Figure 6(b) shows numerous smaller particles with sizes of about 2–3 nm in diameter dispersed within the matrix. The interface can be clearly identified; however, crevices seem undetectable at the interface, indicating an excellent interfacial bonding between the CDHA and PAA-450000 matrix. This enlarged micrograph strongly evidences the good dispersion of the nanoparticles as aforementioned, and the optical transparency of the resulting nanocomposite provides a supporting evidence for the successful two-step synthetic scheme developed in this work.

CONCLUSIONS

Colloidal apatite nanosphere with 2–5 nm in diameter was synthesized in the presence of PAA polyelectrolyte. The PAA polyelectrolyte is successfully acting as a structural-directing agent upon the synthesis of the CDHA nanoparticles. Experimental observation indicates that there exists a critical amount of the PAA polyelectrolyte, above which the morphological evolution from needlelike to spherical was observed. A stable, optically clear, and well-dispersed CDHA suspension can be obtained. By mixing with the high-molecular-weight PAA polymer solution, PAA-CDHA nanocomposites are easily produced. The exceptional uniformity in the distribution of the resulting nanospheres within the PAA matrix suggests outstanding chemical and physical homogeneity, which, in turn, can virtually be considered as a new type of biomaterials. Such an outstanding homogeneity is essentially a breakthrough of the synthetic process employed in this study as compared to those reported in the literature, and may be adopted to further explore new biomaterials of next generation. It is also suggested that the CDHA-PAA nanocomposite developed in this study can be potentially applied for a number of biomedical applications, particularly in the areas of drug delivery and bone tissue engineering, as a result of its nanostructured feature of the resulting matrix phase combined with the bioactive character of the nanoparticulate apatitic phase.

The authors thank ApaMatrix Technologies Incorporated, Canada, for technical support.

REFERENCES

1. Hench LL. Bioceramics: from concept to clinic. J Am Ceram Soc 1991;74:1487–1510.
2. Otsuka M, Matsuda Y, Hsu J, Fox JL, Higuchi W. Mechanochemical synthesis of bioactive material: effect of environmental conditions on the phase transformation of calcium phosphates during grinding. Biomed Mater Eng 1994;4:357–362.
3. Kim W, Zhang Q, Saito F. Mechanochemical synthesis of hydroxyapatite from $Ca(OH)_2$-P_2O_5 and CaO-$Ca(OH)_2$-P_2O_5 mixtures. J Mater Sci 2000;35:5401–5405.

4. Yeong KCB, Wang J, Ng SC. Mechanochemical synthesis of nanocrystalline hydroxyapatite from CaO and $CaHPO_4$. Biomaterials 2001;22:2705–2712.
5. Mortier A, Lemaitre J, Rodrique L, Rouxhet PG. Synthesis and thermal behavior of well-crystallized calcium-deficient phosphate apatite. J Solid State Chem 1989;78:215–219.
6. Vallet-Regi M, Rodriguez-Lorenzo LM, Salinas AJ. Synthesis and characterization of calcium deficient apatite. Solid State Ionic 1997;101–103:1279–1285.
7. Liu DM, Troczynski T, Tseng WJ. Water-based sol–gel synthesis of hydroxyapatite: process development. Biomaterials 2001;22:1721–1730.
8. Liou SC, Chen SY. Transformation mechanism of different chemically precipitated apatitic precursors into β-tricalcium phosphate upon calcinations. Biomaterials 2002;23:4541–4547.
9. Liou SC, Chen SY, Lee HY, Bow JS. Structural characterization of nano-sized calcium deficient apatite powders. Biomaterials 2004;25:189.
10. Kato K, Eika Y, Ikada Y. *In-situ* hydroxyapatite crystallization for the hydroxyapatite/polymer composites. J Mater Sci Mater Med 1997;32:5533–5543.
11. Yamaguchi, Tokuchi K, Fukuzaki H, Koyama Y, Takakuda K, Monma H, Tanaka J. Preparation and microstructure analysis of chitosan/hydroxyapatite nanocomposites. J Biomed Mater Res 2001;50:20–27.
12. Liu Q, De Wijn JR, Van Blitterswijk CA. Nano-apatite/polymer composites: mechanical and physicochemical characterization. Biomaterials 1997;18:1263–1270.
13. Bao Y, Senos AMS, Almeida M, Gauckler LJ. Rheological behavior of aqueous suspensions of hydroxyapatite (HAP). J Mater Sci Mater Med 2002;13:639–643.
14. Hackley VA. Colloidal processing of silicon nitride with poly-(acrylic acid): I. Adsorption and electrostatic interactions. J Am Ceram Soc 1997;80:2315.
15. Liou SC, Chen SY, Liu DM. Synthesis and characterization of needlelike apatitic nanocomposite with controlled aspect ratios. Biomaterials 2003;24:3981–3988.
16. Liou SC, Chen SY, Liu DM. Manipulation of phase development and structural characterization of calcium phosphate ceramics-polyacrylic acid nanocomposites at room temperature in water-methanol mixtures. J Mater Sci Mater Med. Forthcoming.